文章编号: 1001 - 9014(2017)01 - 0015 - 05 DOI:10.11972/j.issn.1001 - 9014.2017.01.004

Wavelength calibration of a new monolithically integrated spectral sensor

ZHANG Ya-Guang[1,2], ZHUANG Xin-Gang[1,3,4], WANG Xu-Quan[1,2], LIU Jun-Liang[1,3], FANG Jia-Xiong[1,5], SHAO Xiu-Mei[5*], WANG Li-Li[1,4*]

(1. Advanced Research Center for Optics, Shandong University, Jinan 250100, China;
2. State Key Laboratory of Crystal Materials, Shandong University, Jinan 250100, China;
3. School of Information Science and Engineering, Shandong University, Jinan 250100, China;
4. State Key Laboratories of Transducer Technology, Shanghai Institute of Microsystem and Information Technology, Chinese Academy of Sciences, Shanghai 200050, China;
5. State Key Laboratories of Transducer Technology, Shanghai Institute of Technical Physics, Chinese Academy of Sciences, Shanghai 200083, China)

Abstract: A new near-infrared monolithically integrated multichannel spectral sensor (MCSS) serves as a key component of Spectral-sensing Internet of Things (SSIOT). A wavelength calibration method for the MCSS was proposed. The method is based on the relative spectral response and includes specific principles of wavelength allocation. Several pixels comprised a channel with the calibrated wavelength. Experimental tests were conducted in the calibrated MCSS and other two commercial spectrometers. The compared spectrum results demonstrated calibration accuracy of 1.8 nm on average, with performance as good as a commercial spectrometer equipped with similar FWHM and sampling intervals, which can meet the application demand.

Key words: shortwave infrared, monolithically integrated spectral sensor, wavelength calibration, spectral-sensing Internet of Things

PACS: 06.20.fb, 07.57.Ty

一种新型单片集成光谱传感器的波长定标方法

张亚光[1,2], 庄新港[1,3,4], 王绪泉[1,2], 刘俊良[1,3], 方家熊[1,5], 邵秀梅[5*], 王丽丽[1,4*]

(1. 山东大学 光学高等研究中心,山东 济南 250100;
2. 山东大学 晶体材料国家重点实验室,山东 济南 250100;
3. 山东大学 信息科学与工程学院,山东 济南 250100;
4. 中国科学院上海微系统与信息技术研究所 传感技术联合国家重点实验室,上海 200050;
5. 中国科学院上海技术物理研究所 传感技术联合国家重点实验室,上海 200083)

摘要:新型短波红外单片集成光谱传感器(MCSS)是光谱传感物联网的核心感知部件.提出了一种 MCSS 的波长定标方法,根据相对光谱响应度和波长分配原则把相邻像素组成一个定标通道.分别采用 MCSS 和两款商用光谱仪测量标准物质的光谱.实验结果表明,平均定标偏差为 1.8 nm,与一款具有相似 FWHM 和取样间隔的商用光谱仪接近,能够满足实际应用的需要.

关 键 词:短波红外;单片集成光谱传感器;波长定标;光谱传感物联网

中图分类号:TB96; O433.1 **文献标识码**:A

Received date: 2016-04-12, **revised date**: 2016-04-14 **收稿日期**:2016-04-12, **修回日期**:2016-04-14

Foundation items: Supported by the National Nature Science Foundation of China (61376052); the Project of State Key Laboratories of Transducer Technology (SKT1507)

Biography: ZHANG Ya-guang (1990-), male, Jinan, master. Research area involves spectral sensors. E-mail: zygssdfx0619@sina.com

* **Corresponding author**: E-mail: shaoxm@mail.sitp.ac.cn; wanglili1983@sdu.edu.cn

Introduction

Spectral-sensing Internet of Things (SSIOT) is a complementarily technological integration of near-infrared (NIR) spectroscopic analysis and communication networks. It can offer nondestructive, accurate and real-time composition-analysis results of detected objects thanks to the spectroscopic analysis[1-4]. Additionally, it also can transfer the useful data to users instantly via the advanced communication network which is attributed to the conventional Internet of Things[5-7]. Therefore, the SSIOT has a variety of potential applications in the field of agriculture, industry, environmental protection, medical treatment and others[8-11].

Serving as a core component of the SSIOT, the spectroscopic sensor has changed from a laboratory curiosity to being qualified for the outdoor condition which is affected inevitably by changeable temperature, humidity, and even frequent vibration. Accordingly, it requires miniaturization, stability, and low-power consumption as the distinguishing features of the sensor. Therefore, a monolithically integrated multichannel spectral sensor (MCSS) is presented, which has rarely been reported before. The MCSS comprises three main components: 1) a multichannel integrated narrowband filter array; 2) a 128-array uncooled InGaAs detector; 3) a readout circuit chip. As to the multichannel integrated filter array, the central wavelength of each filter channel varies with the position along the length of the filter array. Thus the incident light is separated into distinct monochromatic lights along with the direction. Although an optical filter array of this kind was developed by Wang *et al*[12], it did not cover the shortwave infrared range. For applications in this range, a new MCSS (Fig. 1), with a designed sampling interval of 5 nm, has been developed by Shanghai Institute of Technical Physics of the Chinese Academy of Science (SITP).

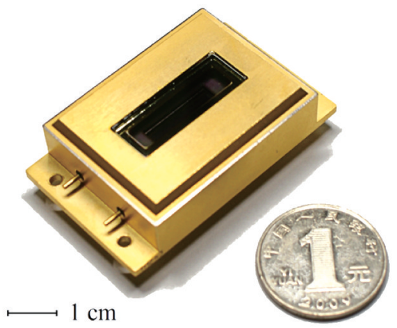

Fig. 1 Photograph of the new monolithically integrated multichannel spectral sensor (MCSS) and a one RMB coin (in the lower right corner)

图 1 新型单片集成光谱感知组件照片(右下角为 1 元 RMB)

In order to obtain reliable detection or analysis results and then to apply the MCSS into the field of spectroscopic analysis[13-14], the MCSS needs calibrating rigorously. Normally, for conventional spectrometers such as grating ones, polynomial fitting is a widely-used method and needs the sufficient number of distributed standard emission or absorption lines in the calibrated spectrum range. However, that sometimes cannot meet high-accuracy calibration due to the lack of specific standard lamps or materials. So some researches employed advanced optical devices such as waveguide comb filter[15] and white light spectral interferometry[16] to support more available standard lines. Also, by studying the system parameters for calibrated spectrometer[17-18], more reliable and accurate calibration relationship between wavelengths and pixels could be deduced. Yet, to our knowledge, these approaches have not been used to calibrate the MCSS. Previous researches about new-type spectroscopic sensors emphasize the results of optical performance, especially the relative spectral response (RSR)[19-20]. Nevertheless, details about both the process of calibration and the spectra of objects detected by these sensors are rarely given.

To address the above calibration issues, a method for calibrating the MCSS was introduced based on the RSR results. Spectra collected by this device and other two commercial spectrometers were compared to test the calibration accuracy. This work enables the MCSS to measure spectra of objects accurately.

1 Wavelength calibration

The calibration method mainly depends upon the RSR results of the MCSS, which are obtained by the spectral comparator. This testing system has been previously described in detail[21-24]. Briefly, the system incorporates four main components: a 500 mm focal length monochromator (Omni-λ500, Zolix, China) that was calibrated before measurement, a standard pyroelectric detector, a tungsten halogen lamp and a translation stage.

During the process of calibrating wavelengths of each channel, three fundamental principles are considered apart from the RSR: 1) Pixels with the same or close peak response wavelength are combined for a channel, with 1 nm tolerance for differences between close peak wavelengths; 2) the calibrated wavelength of each channel is the mean value of peak wavelengths of all pixels belonging to the same channel; 3) the wavelength interval between adjacent channels is within a tolerance of an interval difference of 1 nm. It is true that the first and third principle are mutually restricted sometimes, which needs wavelength rearrangement between pixels and channels with a different tolerance. However all of those are formulated for increasing both the smoothness of measured spectra and the repeatability of measurement. After calibration process, the calibration accuracy was tested by two standards-an optical glass filter (doped by 5% Sm_2O_3) and a laser diode (LD). The spectrum results were measured by three separate devices: the MCSS, an optical spectrum analyzer (AQ6370C, YOKOGAWA, Japan) and a spectrometer (AvaSpec-NIR256-2.5TEC, AVANTES, the Netherlands). Those two widely-used commercial devices were calibrated before measurement.

2 Results and discussion

Figure 2 presents the RSR ranging from 1355 nm to

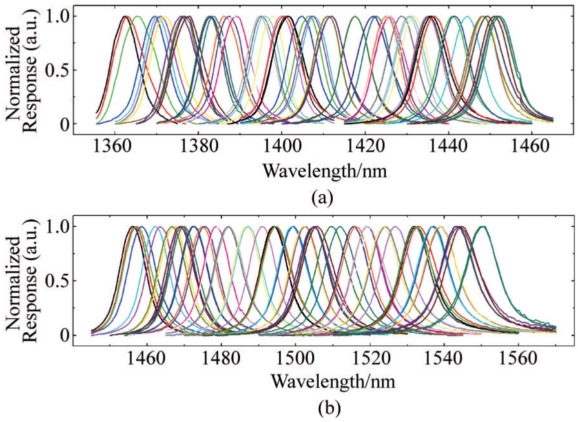

Fig. 2 Relative spectral responsivity of each pixel within the MCSS: (a) NO. 1 to NO. 67 pixels except dead pixels: NO. 1, NO. 3 and NO. 4 pixels; (b) NO. 68 to NO. 128 pixels. Each curve represents the responsivity of a pixel. The position of the responsivity curves moves towards longer wavelength with ordinal number of pixels increasing

图 2 MCSS 各像素的相对光谱响应度:(a)NO. 1 至 NO. 67 像素,除 NO. 1,NO. 3 和 NO. 4 三个坏元;(b) NO. 68 至 NO. 128 像素,每条曲线代表一个像素,随像素序号增加,光谱响应度曲线往长波方向移动

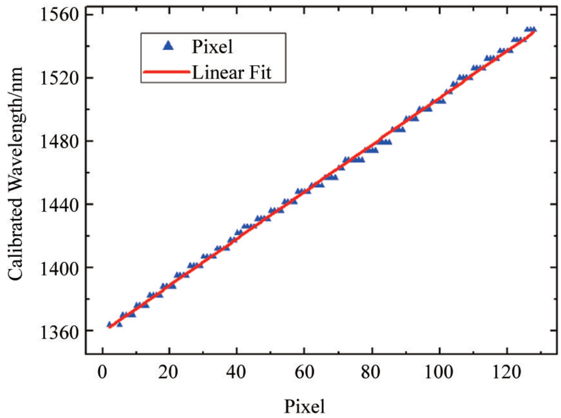

Fig. 3 Calibration results of the whole pixels

图 3 像素波长标定结果

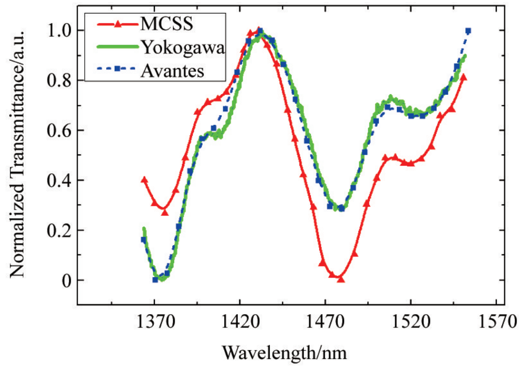

Fig. 4 Transmittance spectra of an optical filter measured by Avantes, MCSS, and Yokogawa

图 4 滤光片透过率的测量结果. 三种测量设备分别为 Avantes, MCSS 和 Yokogawa

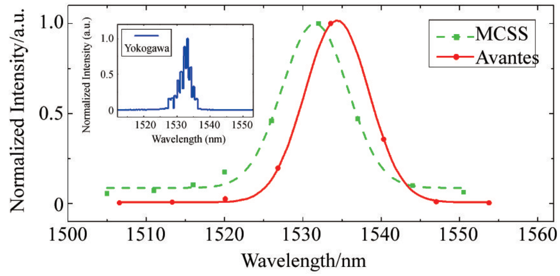

Fig. 5 Spectra of an infrared laser diode (LD) measured by Avantes, MCSS, and Yokogawa

图 5 红外激光二极管光谱的测量结果. 三种测量设备分别为 Avantes, MCSS 和 Yokogawa

1565 nm. The FWHM (full width at half maximum) of each pixel distributes between 7.5 nm and 11.5 nm. The distribution of peak response wavelength is not uniform or linear enough as desired, which is evidenced by two aspects. Firstly, not merely two but more (3, 4 or even 5) adjacent pixels have similar spectral characteristics. Second, the wavelength interval between two adjacent channels varies from 3 nm to 6 nm, instead of equally fixing on the original design of 5 nm. These two unexpected results can be explained by two main reasons: 1) During the process of manufacturing the MCSS, some uncontrollable factors affect its performance negatively[12]; 2) the wavelength of the monochromator employed in the spectral comparator is not accurate enough. To solve the problem of non-uniformity, several adjacent pixels form a new channel, as long as the maximum deviation between peak response wavelengths of those pixels is less than 2.5 nm (half of the designed sampling interval). Also, every wavelength interval is controlled around 5 nm, with the tolerance that is given in principle 3) relaxed to 2 nm. Needless to say, certain solutions comply with the principles of this calibration method as far as possible and, meanwhile, are inevitably at the cost of the calibration accuracy to some extent.

The calibration results of all pixels allocated to 34 different channels are demonstrated in Fig. 3. Generally, one channel contains four pixels, while channels with two or six pixels occur occasionally. It is not recommended that a channel consists of only one pixel, since the size of a single pixel is too small to have high measurement repeatability. In addition, the modified wavelength interval ranges from 4 nm to 8 nm and mainly focus on 5 nm. Thus, it is evident from Fig. 3 that the wavelength distribution is nearly linear.

As shown in Fig. 4 and Fig. 5, the overall trend of spectra measured by the MCSS approximates to that measured by the others well. Moreover, wavelengths of these spectra's peaks and bottoms and corresponding measurement deviations are illustrated in Table 1. Reference standards in the brackets were obtained by Yokogawa, because of its high accuracy and precision. For the MCSS, the minimum wavelength deviation is negligibly-0.8 nm at Bottom 2, while the maximum one is -3.0 nm at Peak 2. This seemingly deficient occurrence results from calibrated wavelengths of the two adjacent channels around Peak 2. In front of the 1511-nm channel, the nearby one is calibrated to 1505 nm. By coincidence, Peak 2 of 1508 nm lies at the central of the two channels precisely. Thus, the location of Peak 2-1511 nm-measured by the MCSS is not incorrect but reasonable, which indicates an intrinsic performance of the MCSS. Modifying this wavelength towards a shorter value can lead to measurement errors existing in the next sampling interval from 1511 nm to 1516 nm. Equipped with a similar FWHM (the nominal minimum of 6.0 nm) and sampling intervals (nominal 5.9 nm on average), Avantes generates a relatively larger deviation of 3.9 nm in Bottom 1 by comparison. It was also found that the mean deviation of the MCSS is 1.8 nm which is merely 0.2 nm more than that of Avantes. The calibration accuracy of 1.8 nm on average is 29.1% of the mean sampling interval and 24.0% of the minimum FWHM. Avantes, by contrast, has two similar results: 27.1% and 26.7%, respectively. In consequence, the calibration is feasible and competent to some spectroscopic applications.

In terms of the absolute transmittance illustrated in Fig. 4, it is impossible that three devices can provide us with the identical results, simply because the performance of InGaAs detectors installed in separate equipment differs greatly due to different working temperature of detectors[25]. Moreover, the accuracy of 1.8 nm is possibly not enough for some high-accuracy applications, so that the calibration method based on rigorous mathematics should be worked out. However, the mathematics method leads to complex classified discussion about the wavelength interval and the number of pixels within a channel. In contrast, our method without complicated mathematic computation is not only relatively simple but also effective. In the future, improvements of the MCSS will be carried on to simplify the calibration method and realize higher accuracy.

3 Conclusion

In conclusion, the wavelength of the versatile MCSS was calibrated, which was a crucial premise for applying this MCSS and for spectroscopic analysis. With the FWHM of each pixel distributing between 7.5 nm and 11.5 nm, the spectral region of the MCSS ranges from 1355 nm to 1565 nm. The calibration accuracy is tested to be 1.8 nm on average. By comparing the measurement results, the MCSS presents comparable performance with a commercial spectrometer-Avantes. The results confirm that the calibration method is effective and qualified to spectroscopic analysis. It would be beneficial to study not only the more accurate but also more complicated calibration method based on rigorous mathematics.

References

[1] Nichols P D, Henson J M, Guckert J B, *et al*. Fourier transform-infrared spectroscopic methods for microbial ecology: analysis of bacteria, bacteri-polymer mixtures and biofilms [J]. *Journal of microbiological methods*, 1985, 4(2): 79-94

[2] Luypaert J, Zhang M, Massart D. Feasibility study for the use of near infrared spectroscopy in the qualitative and quantitative analysis of green tea Camellia sinensis (L.) [J]. *Analytica Chimica Acta*, 2003, **478**(2): 303-12

[3] Zhang M, Luypaert J, Pierna J F, *et al*. Determination of total antioxidant capacity in green tea by near-infrared spectroscopy and multivariate calibration [J]. *Talanta*, 2004, **62**(1): 25-35

[4] Kong J, Yu S. Fourier transform infrared spectroscopic analysis of protein secondary structures [J]. *Acta biochimica et biophysica Sinica*, 2007, **39**(8): 549-59

[5] Gubbi J, Buyya R, Marusic S, *et al*. Internet of Things (IoT): A vision, architectural elements, and future directions [J]. *Future Generation Computer Systems*, 2013, **29**(7): 1645-60

[6] Lee I and Lee K. The Internet of Things (IoT): Applications, investments, and challenges for enterprises [J]. *Business Horizons*, 2015, **58**(4): 431-40

[7] Nguyen K T, Laurent M, Oualha N. Survey on secure communication protocols for the Internet of Things [J]. *Ad Hoc Networks*, 2015, 32: 17-31

[8] Burns D A and Ciurczak E W. Handbook of near-infrared analysis [M]. Boca Raton: CRC Press, 2007, 23-4

[9] Roggo Y, Chalus P, Maurer L, *et al*. A review of near infrared spectroscopy and chemometrics in pharmaceutical technologies [J]. *Journal of pharmaceutical and biomedical analysis*, 2007, **44**:683-700.

[10] Siesler H W, Ozaki Y, Kawata S, *et al*. Near-infrared spectroscopy: principles, instruments, applications [M]. Hoboken John: Wiley & Sons, 2008, 32-3.

[11] Weber R H, Weber R. Internet of Things [M]. Berlin: Springer, 2010, 25-7.

[12] Wang Z, Sang T, Wang L, *et al*. Narrowband multichannel filters and integrated optical filter arrays [J]. *Applied Optics*, 2008, **47**(13): C1-C8.

[13] Asimellis G, Giannoudakos A, Kompitsas M. Accurate wavelength calibration in the near-infrared for multielement analysis without the need for reference spectra [J]. *Applied Optics*, 2006, **45**(35): 8855-62.

[14] Mohamed T N, South A, Newnham D, *et al*. A new accurate wavelength calibration for the ozone absorption cross section in the near-UV spectral region, and its effect on the retrieval of BrO from measurements of zenith-scattered sunlight [J]. *Journal of Geophysical Research: Atmospheres*, 2001, **106**(D9): 9897-907.

[15] Yu Z, Huang M, Wang Y, *et al*. Fast wavelength calibration method for spectrometers based on waveguide comb optical filter [J]. *Review of Scientific Instruments*, 2015, **86**(4): 043103-6.

[16] de la Fuente R. White Light Spectral Interferometry as a Spectrometer Calibration Tool [J]. *Applied spectroscopy*, 2014, **68**(5): 525-530.

[17] Xiong G, Zhang J, Yang G, *et al*. Different approaches to precise wavelength calibration of a flat-field grating spectrometer for laser-produced plasmas [J]. *Physica Scripta*, 2014, **89**(6): 065005-9.

表1 Avantes和MCSS的波长测量偏差. 以滤光片透过率的峰值和波谷以及红外LD峰值波长为参考点. 平均偏移量为各偏差绝对值的平均. 波长单位为nm

Table 1 Wavelength deviations of Avantes and the MCSS, relating to the peak and bottom wavelengths of the optical filter's transmittance and infrared LD. All the wavelengths are in units of nm

Devices	Bottom 1 (1374.4)	Peak 1 (1432.8)	Bottom 2 (1478.2)	Peak 2 (1478.2)	Bottom 3 (1518.0)	LD Peak (1533.4)	Mean deviations
Avantes	−1.7	1.9	−0.8	−3.0	−2.0	1.3	1.8
MCSS	3.9	0.8	−1.3	1.4	−2.1	−0.2	1.6

[18] Liu K , Yu F. Accurate wavelength calibration method using system parameters for grating spectrometers [J]. *Optical Engineering*, 2013, **52**(1): 013603-6.

[19] Emadi A, Wu H, Grabarnik S, *et al*. Fabrication and characterization of IC-Compatible Linear Variable Optical Filters with application in a micro-spectrometer [J]. *Sensors and Actuators A: Physical*, 2010, **162**(2): 400-5.

[20] Keating A, Antoszewski J, Silva K, *et al*. Design and characterization of Fabry-Perot MEMS-based short-wave infrared microspectrometers [J]. *Journal of electronic materials*, 2008, **37**(12): 1811-20.

[21] Friedrich R, Fischer J , Stock M. Accurate calibration of filter radiometers against a cryogenic radiometer using a trap detector [J]. *Metrologia*, 1995, **32**(6): 509-13.

[22] Lu X, Yuan Z, Hao X, *et al*. Calibration of the Irradiance, Responsivity of a Filter Radiometer for T Measurement at NIM International [J]. *Journal of Thermophysics*, 2011, **32**(1-2): 278-84.

[23] Campos J, Corróns A, Pons A, *et al*. Spectral responsivity uncertainty of silicon photodiodes due to calibration spectral bandwidth [J]. *Measurement Science and Technology*, 2001, **12**(11): 1926-31.

[24] Lamminpää A, Noorma M, Hyyppä T, *et al*. Characterization of germanium photodiodes and trap detector [J]. *Measurement Science and Technology*, 2006, **17**(4): 908-12.

[25] Rogalski A. Progress in focal plane array technologies [J]. *Progress in Quantum Electronics*, 2012, **36**(2): 342-473.

(上接 14 页)

[11] Hirori H, Yamashita K, Nagai M, *et al.* Attenuated Total Reflection Spectroscopy in Time Domain Using Terahertz Coherent Pulses[J]. Japanese Journal of Applied Physics, 2004, **43**(10A):361-363.

[12] Duvillaret L, Garet F, Coutaz J L. Influence of noise on the characterization of materials by terahertz time-domain spectroscopy [J]. J. Opt. Soc. Amer. B, 2000, **17**(3): 452-461.

[13] Withayachumnankul W, Fischer B M, Lin H, *et al.* Uncertainty in terahertz time-domain spectroscopy measurement[J]. Journal of the Optical Society of America B, 2008, **25**(6):1059-1072.

[14] Lin H, Mickan S P, Fischer B M, *et al.* Analysis of measurement uncertainty in THz-TDS[J]. Proceedings of SPIE-The International Society for Optical Engineering, 2007, 6593.

[15] Soltani A, Probst T, Busch S F, *et al*. Error from Delay Drift in Terahertz Attenuated Total Reflection Spectroscopy [J]. Journal of Infrared Millimeter & Terahertz Waves, 2014, **35**(5):468-477.

[16] Yang Fei, Liu Li-Ping, Song Mao-jiang, *et al*. Uncertainty in Terahertz time-domain spectroscopy measurement of liquids[J]. J Infrared Milli Terahz Waves, 2017, **38**(2): 229-247.

[17] Hangyo M, Nagashima T, Nashima S. Spectroscopy by pulsed terahertz radiation[J]. Measurement Science & Technology, 2002, **13**(13):1727-1738.

[18] Khazan M, Meissner R, Wilke I. Convertible transmission-reflection time-domain terahertz spectrometer [J]. Review of Scientific Instruments, 2001, **72**(8): 3427-3430.

[19] Vartiainen E M, Ino Y, Shimano R, *et al.* Numerical phase correction method for terahertz time-domain reflection spectroscopy[J]. Journal of Applied Physics, 2004, **96**(8):4171-4175.

[20] Duvillaret L, Garet F, Roux J F, *et al.* Analytical modeling and optimization of terahertz time-domain spectroscopy experiments, using photoswitches as antennas[J]. IEEE Journal of Selected Topics in Quantum Electronics, 2001, **7**(4):615-623.

[21] Gürtler A, Winnewisser C, Helm H, *et al*. Jepsen, Terahertz pulse propagation in the near field and the far field[J]. J. Opt. Soc. Am. A, 2000, **17**,74-83.